Blue Copper Models. Synthesis and Characterization of Copper(II) Enethiolate Complexes derived from (1*R*)-3-Hydroxymethylenebornane-2-thione and 2-Aminothia-alkyl-1-methylbenzimidazoles (Donor Set N_2SS^*) or Diamines (Donor Set N_2S_2)

Luigi Casella, Michele Gullotti, and Edoardo Suardi
Dipartimento di Chimica Inorganica e Metallorganica, Centro CNR, Università di Milano, Via Venezian 21, 20133 Milano, Italy
Massimo Sisti and Roberto Pagliarin
Dipartimento di Chimica Organica e Industriale, Università di Milano, Via Golgi 19, 20133 Milano, Italy
Piero Zanello
Dipartimento di Chimica, Università di Siena, Pian dei Mantellini 44, 53100 Siena, Italy

A series of tetradentate ligands derived from the condensation of (1*R*)-3-hydroxymethylenebornane-2-thione and several 2-aminothia-alkylbenzimidazoles were synthesized together with their cationic zinc(II) and copper(II) complexes. While the free ligands exist in the thioxoenamine tautomeric form, binding to the metals occurs in their enethiolateimine form, as deduced from cumulative spectral evidence. The copper(II) complexes exhibit medium-intensity absorptions between 410 and 435 ($\varepsilon \gtrsim 3\,500$) and between 520 and 535 nm ($\varepsilon \gtrsim 1\,200$ dm^3 mol^{-1} cm^{-1}) attributable to enethiolate $\sigma(S^-) \longrightarrow Cu^{II}$ and $\pi(S^-) \longrightarrow Cu^{II}$ ligand-to-metal charge transfer (l.m.c.t.) transitions, respectively, and relatively intense ligand-field transitions in the range 610—650 nm ($\varepsilon \gtrsim 1\,500$ dm^3 mol^{-1} cm^{-1}). All the bands undergo progressive red shifts as the length of the carbon chain connecting the imine and thioether functions increases from two to four atoms. The frozen-solution e.p.r. spectra are indicative of progressive distortion towards a pseudo-tetrahedral geometry for copper(II) as the carbon chain length increases. A series of neutral copper(II) complexes derived from the condensation of (1*R*)-3-hydroxymethylenebornane-2-thione and symmetric diamines was also synthesized for comparison. Here too the length of the carbon chain connecting the imine nitrogen atoms was varied from two to four atoms. These complexes exhibit the same spectroscopic trends but with less marked distortion of the copper(II) chromophores as the length of the carbon chain increases. The cationic copper(II) complexes from (1*R*)-3-hydroxymethylenebornane-2-thione and 2-aminothia-alkylbenzimidazoles display, in acetonitrile solution at −15 °C, easy access to the corresponding copper(I) congeners ($E^0 = -0.02$ V *vs.* s.c.e.). By contrast, the neutral copper(II) species derived from (1*R*)-3-hydroxymethylenebornane-2-thione and diamines are reduced to the corresponding copper(I) complexes at potentials more negative by 0.7—1.0 V, depending upon the extent of stereochemical distortion around the copper(II) centre induced by the length of the imine-nitrogen-linking carbon chain. The planar complex bearing an ethylene bridging chain can be reversibly oxidized to the corresponding copper(III) species ($E^0 = +0.37$ V).

Our approach to the modelling of the active sites of blue copper proteins involves the development of synthetic routes to new polydentate ligand systems containing sterically protected thiol groups and imine, imidazole, and thioether groups. These groups should simulate the ligand environment of the copper blue sites.[1] Steric protection of the thiol group is essential in synthetic copper(II) complexes in order to prevent the easy redox process leading to copper(I) and disulphide.[2,3] More serious is the problem of building a rigid ligand molecule with the above donor groups that can impose a pseudotetrahedral geometry on copper(II). Low-molecular-weight compounds cannot reproduce properties of the blue sites that arise from the protein backbone.

In previous papers we reported the synthesis of several copper(II) complexes (**1**) and (**2**) with imine ligands obtained from the condensation of 1-substituted 3-formyl-2(1*H*)-pyridinethione (**3**) and a series of 2-aminothia-alkyl-imidazole or -benzimidazole derivatives.[4] The main object of that work was to identify a general strategy to obtain suitable polyfunctional ligand molecules. The length of the carbon chains R and R^1 and the nature of the pyridine substituent R^2 were investigated. The pyridinethione residue was used as a mimic for the cysteine thiolate because of the pyridinium thiolate character that it assumes when bound to a metal ion,[4a,5] so that the higher redox stability of heterocyclic thiols could be exploited, as has often been done in synthetic copper biomimetic chemistry.[6] The parent bis(imine) complexes of types (**4**) and (**5**) have also been characterized separately.[7]

We report here an improved model system that more faithfully mimics cysteine thiolate co-ordination in the proteins. This involves bonding of the α,β-unsaturated thiolate form of the ligands (**8**) to Cu^{II} and Zn^{II}, as shown in (**9**). The ligands (**8**) result from condensation between (**6**) and a series of compounds (**7**). To our knowledge the copper(II) systems (**9**) are the first biomimetic models with N_2SS^* donor ligands carrying an overall monopositive charge. The parent copper(II) complexes (**11**) derived from the N_2S_2 ligands (**10**), resulting from the condensation of symmetric diamines and two molecules of (**6**), are also reported for comparison.

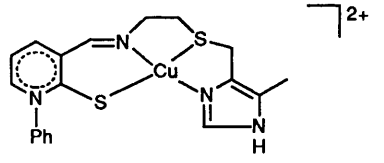

(1)

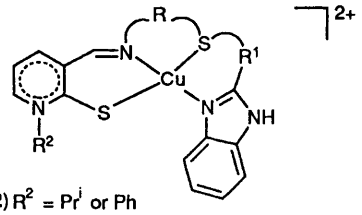

(2) R^2 = Pr^i or Ph
R^1 = CH_2 or $(CH_2)_2$
R = $(CH_2)_2$, $(CH_2)_3$ or $(CH_2)_4$

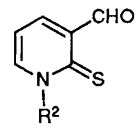

(3) R^2 = Pr^i or Ph

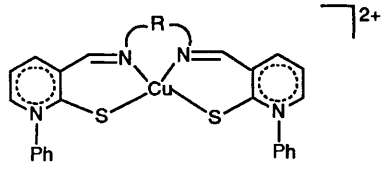

(4) R = $(CH_2)_2$,$(CH_2)_3$, or $(CH_2)_4$

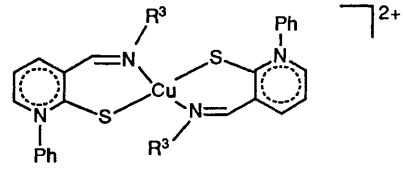

(5) R^3 = Bu^n, Bu^s, 4 – MeC_6H_4, or 3 – $O_2NC_6H_4$

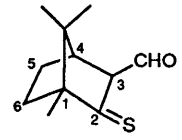

(6)

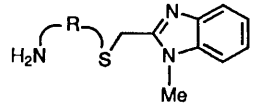

(7) R = $(CH_2)_2$, $(CH_2)_3$, or $(CH_2)_4$

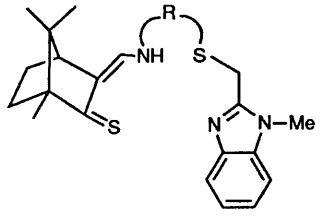

(8) HL^1 R = $(CH_2)_2$
HL^2 R = $(CH_2)_3$
HL^3 R = $(CH_2)_4$

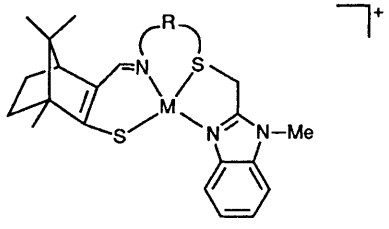

(9) R = $(CH_2)_2$, $(CH_2)_3$, or $(CH_2)_4$

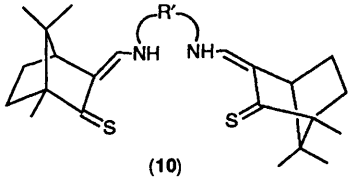

(10)

H_2L^4 R′ = $(CH_2)_2$
H_2L^5 R′ = $(CH_2)_3$
H_2L^6 R′ = CH_2–CH_2

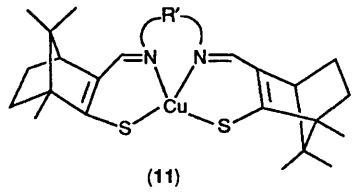

(11)

Experimental

Physical Measurements.—Elemental analyses were by the microanalytical laboratory of our Department. Infrared spectra were recorded with a Nicolet MX-1E FT instrument, electronic spectra on a HP 8452 diode-array spectrophotometer, circular dichroism (c.d.) spectra with a Jasco J-500C dichrograph, proton n.m.r. spectra at 80 or 200 MHz on Bruker WP-80 or AC-200 spectrometers (all chemical shift data are referenced to $SiMe_4$), and e.p.r. spectra on frozen solutions of the complexes at *X*-band frequencies using a Varian E-109 instrument. Materials and cells for electrochemical tests have been described elsewhere.[4b] Either a BAS 100A electrochemical analyzer or a multipurpose Amel instrument (a model 566 analogue function generator and a model 552 potentiostat) was used as a polarizing unit. Controlled-potential coulometry at low temperature (−15 °C) was performed by using an Ag–AgCl reference electrode. All the potentials reported refer to the saturated calomel electrode (s.c.e.). The ferrocenium–ferrocene couple exhibited potentials of +0.35 at −15 and +0.38 V at +18 °C.

Reagents and Preparations.—*N*-Methyl-*o*-diaminobenzene (Kodak), the *N*-bromoalkylphthalimides, and the Lawesson reagent, 2,4-bis(4-methoxyphenyl-2,4-dithio-1,3,2,4-dithiadiphosphetate (Fluka) were commercially available; all other reagents were of the highest grade available and were used as received. Toluene and diethyl ether were dried by refluxing over and distillation from metallic sodium.

2-*Mercaptomethyl*-1-*methylbenzimidazole* (**12**) *hydrochloride*. *N*-Methyl-*o*-diaminobenzene (30.8 mmol) and mercaptoacetic acid (36.9 mmol) were refluxed in 6 mol dm^{-3} aqueous hydrochloric acid (40 cm^3) for about 50 h. The green solution thus obtained was concentrated under vacuum until a white precipitate formed. After cooling the precipitate was filtered off, washed with diethyl ether, and crystallized from methanol (yield 70%). A small sample of the free base for recording the n.m.r. spectrum was obtained by addition of a stoicheiometric amount of sodium hydroxide in methanol, evaporation to dryness, and extraction with chloroform. ^1H N.m.r. ($CDCl_3$): δ 7.8—7.5, 7.3—7.0 (m, 4 H, Ph), 3.80 (s, 2 H, CH_2), 3.58 (s, 3 H, CH_3), and 2.15 (s, br, 1 H, SH).

Phthalimides (**13**). Metallic sodium (27.4 mmol) was dissolved in dry ethanol (70 cm^3) under nitrogen. When the evolution of hydrogen gas had ceased, 2-mercaptomethyl-1-methylbenzimidazole (13.7 mmol) was added with stirring. Then, a *N*-bromoalkylphthalimide (13.7 mmol) was added and the mixture heated slowly to reflux temperature. Refluxing was continued for 24 h under an inert atmosphere. After cooling to room temperature an equal volume of dichloromethane was added, the inorganic salts were filtered off, and the filtrate was evaporated to dryness. The residue was dissolved in the minimum amount of chloroform and chromatographed on an alumina column (4 × 40 cm, chloroform as eluant). After elution of a minor band of unreacted bromoalkylphthalimide, the band of (**13**) was collected and concentrated to a light yellow oil. Addition of diethyl ether gave a white solid (yield 75—95%).

1-*Methyl*-2-(4′-*phthalimido*-2′-*thiabutyl*)*benzimidazole* [**13a**; R = $(CH_2)_2$]. I.r. (Nujol mull): 1 768m, 1 715vs, 742m, and 721m cm^{-1}. ^1H N.m.r. ($CDCl_3$): δ 8.0—7.6 (m, 5 H, Ph), 7.4—7.2 (m, 3 H, Ph), 4.09 [s, 2 H, CH_2C(benzimidazole)], 3.91 (t, 2 H, CH_2N), 3.76 (s, 3 H, CH_3N), and 2.88 (t, 2 H, CCH_2S).

1-*Methyl*-2-(5′-*phthalimido*-2′-*thiapentyl*)*benzimidazole* [**13b**; R = $(CH_2)_3$]. I.r. (Nujol mull): 1 770m, 1 720vs, 738m, and 725s cm^{-1}. ^1H N.m.r. ($CDCl_3$): δ 8.0—7.6 (m, 5 H, Ph), 7.4—7.2 (m, 3 H, Ph), 3.92 [s, 2 H, CH_2C(benzimidazole)], 3.77 (s, 3 H, CH_3N), 3.71 (t, 2 H, CH_2N), 2.65 (t, 2 H, CCH_2S), and 2.1—1.7 (m, 2 H, CCH_2C).

1-*Methyl*-2-(6′-*phthalimido*-2′-*thiahexyl*)*benzimidazole* [**13c**; R = $(CH_2)_4$]. I.r. (Nujol mull): 1 768m, 1 713vs, 740m, and 719m cm^{-1}. ^1H N.m.r. ($CDCl_3$): δ 8.0—7.5 (m, 5 H, Ph), 7.4—7.2 (m, 3 H, Ph), 3.92 (s, 2 H, CH_2C(benzimidazole)], 3.80 (t, 2 H, CH_2N), 3.76 (s, 3 H, CH_3N), 2.60 (approximate t, 2 H, CCH_2S), and 1.9—1.4 (m, 4 H, CCH_2C).

2-*Aminothia-alkyl*-1-*methylbenzimidazole* (**7**) *dihydrochlorides*. The phthalimide derivative (**13**) (10.5 mmol), hydrazine dihydrochloride (10.5 mmol), and potassium hydroxide (21.0 mmol) were refluxed in ethanol (70 cm^3) for about 60 h. After cooling to room temperature an equal volume of dichloromethane was added and the mixture cooled in a refrigerator. The white precipitate was filtered off and the filtrate evaporated to dryness. The residue was treated with 6 mol dm^{-3} hydrochloric acid (50 cm^3) and the mixture refluxed for about 60 h. On concentrating under vacuum, a white powder precipitated. This was filtered off and the filtrate taken to dryness under vacuum. The light brown residue was treated several times with ethanol and evaporated to dryness, then refluxed with toluene in a Dean–Stark apparatus filled with molecular sieves on the side arm until a solid white product was obtained (yield 85—95%).

2-(4′-*Amino*-2′-*thiabutyl*)-1-*methylbenzimidazole dihydrochloride* (**7a**)·2HCl [R = $(CH_2)_2$]. ^1H N.m.r. (D_2O): δ 8.0—7.5 (m, 4 H, Ph), 4.43 [s, 2 H, CH_2C(benzimidazole)], 4.04 (s, 3 H, CH_3N), 3.34 (approximate t, 2 H, CH_2N), and 3.01 (approximate t, 2 H, CH_2S).

2-(5′-*Amino*-2′-*thiapentyl*)-1-*methylbenzimidazole dihydrochloride* (**7b**)·2HCl [R = $(CH_2)_3$]. ^1H N.m.r. (D_2O): δ 8.0—7.4 (m, 4 H, Ph), 4.28 [s, 2 H, CH_2C(benzimidazole)], 3.98 (s, 3 H, CH_3N), 3.05 (t, 2 H, CH_2N), 2.68 (t, 2 H, CH_2S), and 2.1—1.8 (m, 2 H, CCH_2C).

2-(6′-*Amino*-2′-*thiahexyl*)-1-*methylbenzimidazole dihydrochloride* (**7c**)·2HCl [R = $(CH_2)_4$]. ^1H N.m.r. (D_2O): δ 8.0—7.5 (m, 4 H, Ph), 4.35 [s, 2 H, CH_2C(benzimidazole)], 4.03 (s, 3 H, CH_3N), 3.0 (m, 2 H, CH_2N), 2.7 (m, 2 H, CH_2S), and 1.9—1.6 (m, 4 H, CCH_2C).

Small amounts of pure free bases (**7**) were prepared as needed according to the following procedure. The dihydrochloride salt of the 2-aminothia-alkyl-1-methylbenzimidazole (1—3 mmol) was treated with the stoicheiometric amount of sodium hydroxide in methanol and the resulting mixture evaporated to dryness. The residue was dissolved in the minimum amount of chloroform and chromatographed on an alumina column (3 × 30 cm) using chloroform–methanol–concentrated ammonia (60:30:5 v/v/v) as eluant. The light brown main central band was collected and carefully evaporated to dryness under vacuum.

(1R)-*Thiocamphor* {(1R)-1,7,7-*Trimethylbicyclo*[2.2.1]-*heptane*-2-*thione*} (**14**). A mixture of (1*R*)-(+)camphor (39.4 mmol), Lawesson reagent (23.7 mmol), and anhydrous toluene (20 cm^3) was refluxed under an inert atmosphere for 5 h. The orange solution so obtained was cooled and evaporated to dryness under vacuum. The residue was dissolved in the minimum amount of dichloromethane and applied to a silica gel column (4 × 40 cm) using dichloromethane–light petroleum (b.p. 35—60°) (1:1 v/v) as eluant. After a fraction of unreacted camphor, the orange fraction of the product was collected and evaporated to dryness (yield 85%). The oil was stored under nitrogen in the cold. Mass spectrum: *m*/*z* (%) 168 (M^+, 100), 153 (42), 139 (12), 135 (17), 126 (32), 125 (80), 119 (12), 113 (75), 112 (53), 95 (54), 93 (44), 91 (36), and 85 (84). I.r. (film): 1 468m, 1 446s, 1 413m, 1 388s, 1 374w, 1 369w, 1 305vs, 1 292m, 1 279s, 1 265s, 1 210s, 1 131s, 1 088m, 1 002m, and 935m cm^{-1}. N.m.r. ($CDCl_3$): ^1H, δ 3.0—2.6 (m, 1 H), 2.48 (approximate s, ≈1 H), 2.3—1.1 (m, 5 H), 1.09 (s, 3 H), 1.03 (s, 3 H), and 0.80 (s, 3 H); ^{13}C (at 50.3 MHz), δ 271.9 (C=S), 69.4 (s), 55.7 (t), 49.1 (s), 45.3 (d), 34.1 (t), 27.4 (t), 20.0 (q), 19.8 (q), and 13.3 (q). U.v.-visible (MeOH), $\lambda_{max.}$/nm (ε/dm^3 mol^{-1} cm^{-1}): 480 (10) and 246 (8 700). C.d. (MeOH), $\lambda_{max.}$/nm (Δε/dm^3 mol^{-1} cm^{-1}): 504 (+0.2), 445 (−0.12), and 243 (−7.3).

(1R)-3-*Formylthiocamphor* (**6**). To a mixture of metallic sodium (34.2 mmol) in anhydrous diethyl ether (10 cm^3) was added dropwise under an inert atmosphere a solution of thiocamphor (34.2 mmol) in dry diethyl ether (50 cm^3) during 0.5 h. The mixture was left to stir for 3 h. Then, a solution of ethyl formate (44.4 mmol) in dry diethyl ether (25 cm^3) was added dropwise in 0.5 h. The mixture was left to stir for 2 h; then it was extracted with three portions of iced water (30 cm^3 each). The aqueous phase was washed twice with diethyl ether (30 cm^3 each) and degassed at a rotary evaporator in order to remove any traces of ether and unreacted ethyl formate. The aqueous solution was acidified to pH 2 with dilute hydrochloric acid giving a yellow-green suspension. This was extracted three times with diethyl ether (35 cm^3 each). Evaporation of the organic phase under reduced pressure gave an oil (yield 20%) which was stored under nitrogen in the cold (Found: C, 67.10; H, 8.30. Calc. for $C_{11}H_{16}OS$: C, 67.30; H, 8.20%). Mass spectrum: *m*/*z* (%) 196 (M^+, 100), 181 (20), 168 (17), 163 (63), 153 (48), 145 (28), 140 (41), 135 (26), 125 (51), 107 (39), 91 (95), and 81 (55). I.r. (film): 1 722w, 1 636w, 1 605s, 1 470m, 1 455m, 1 399s, 1 373m, 1 246m, 1 240m, 1 195m, 1 130m, 1 091m, 1 071m, 830m, 785w, and 766w cm^{-1}. N.m.r. ($CDCl_3$): ^1H, δ 13.17 (d, *J* 12.6, 1 H, C=CHO*H*, *Z*-enol form), 7.32 (d, *J* 12.6, 1 H, C=C*H*OH), 2.48 (d, *J* 3.6 Hz, 1 H, H^4), 2.2—1.1 (m, 4 H, CCH_2C), 1.11 (s, 3 H, CH_3), 0.96 (s, 3 H, CH_3), and 0.76 (s, 3 H, CH_3); ^{13}C, δ 241.3 (C=S), 156.1 (d), 131.6 (s), 68.2 (s), 52.9 (s), 49.9 (d), 32.6 (t), 27.4

(t), 19.8 (q), 19.2 (q), and 11.5 (q). U.v.-visible (MeOH), $\lambda_{max.}$/nm (ε/dm^3 mol^{-1} cm^{-1}): 254 (4 000), 350 (8 750), 370 (sh) (6 300), and 450 (sh) (70). C.d. (MeOH), $\lambda_{max.}$/nm($\Delta\varepsilon$/dm^3 mol^{-1} cm^{-1}): 242 (+3.81), 289 (+0.34), 350 (−1.00), and 480 (−1.21).

Preparation of the Ligands (**8**).—The condensation products between 3-formylthiocamphor and the 2-aminothia-alkyl-1-methylbenzimidazoles were prepared according to the following procedure. A mixture of the free amine derivative (**7**) (3 mmol), 3-formylthiocamphor (3 mmol), anhydrous ethanol (70 cm^3), and dry toluene (30 cm^3) was refluxed for about 4 h under nitrogen in a Dean–Stark apparatus filled with molecular sieves in the side arm. The resulting solution was concentrated to small volume and chromatographed on a silica gel column [3 × 35 cm, chloroform–ethanol (19:1 v/v) as eluant]. After a fraction of unreacted formylthiocamphor, the fraction of the product was collected and evaporated to drynes. This product was further purified on t.l.c. plates (Merck 60 F_{254}) using chloroform–ethanol (20:1 v/v) as eluant and collecting the main yellow band (yield 40—50%).

HL^1 (Found: C, 66.05; H, 7.45; N, 10.35. Calc. for $C_{22}H_{29}N_3S_2$: C, 66.10; H, 7.30; N, 10.5%). Mass spectrum: *m/z* (%) 400 [(M + 1)$^+$, 58], 399 (M^+, 15), 356 (28), 254 (46), 253 (43), 222 (79), 180 (81), 179 (98), 178 (95), 146 (100), 145 (98), and 131 (62). I.r. (film): 3 370br, 3 064w, 2 958m, 2 872w, 1 626s, 1 508w, 1 475m, 1 454m, 1 332w, 1 274w, 1 220w, 1 197m, and 752s cm^{-1}. N.m.r. ($CDCl_3$): ^{1}H δ 11.5 (br m, 1 H, NH), 7.8—7.6 (m, 1 H, Ph–H), 7.4—7.2 (m, 3 H, Ph–H), 6.79 (d, *J* 12.8, 1 H, =CH), 4.00 [s, 2 H, CH_2C(benzimidazole)], 3.83 (s, 3 H, CH_3N), 3.35 (q, *J* 6.4 Hz, 2 H, CH_2N), 2.72 (t, 2 H, CH_2S), 2.5—1.0 (m, 5 H, CCHC + CCH_2C), 1.09 (s, 3 H, CH_3C), 0.90 (s, 3 H, CH_3C), and 0.69 (s, 3 H, CH_3C); ^{13}C, δ 226.3 (C=S), 192.7 (s), 150.7 (s), 147.8 (d), 142.2 (s), 136.4 (s), 127.3 (s), 123.1 (d), 122.5 (d), 119.7 (d), 109.5 (d), 69.7 (s), 67.0 (t), 53.7 (t), 52.9 (q), 51.0 (d), 48.3 (t), 32.7 (t), 30.4 (q), 28.0 (t), 20.0 (q), and 12.5 (q). C.d. (MeOH), $\lambda_{max.}$/nm($\Delta\varepsilon$/dm^3 mol^{-1} cm^{-1}): 252 (+2.45), 394 (+2.27), and 450 (−2.09).

HL^2 (Found: C, 66.60; H, 7.65; N, 10.00. Calc. for $C_{23}H_{31}N_3S_2$: C, 66.80; H, 7.55; N, 10.15%). Mass spectrum: *m/z* (%) 413 (M^+, 19), 268 (29), 235 (11), 179 (63), 146 (100), 145 (46), and 131 (14). I.r. (film): 3 200 (br), 3 060w, 2 958s, 2 874w, 1 630s, 1 508w, 1 473s, 1 458s, 1 332m, 1 274w, 1 220m, 1 199m, and 752s cm^{-1}. ^{1}H N.m.r. ($CDCl_3$): δ 11.5 (br m, 1 H, NH), 7.8—7.6 (m, 1 H, Ph–H), 7.4—7.2 (m, 3 H, Ph–H), 6.81 (d, *J* 12.9, 1 H, =CH), 3.96 [s, 2 H, CH_2C(benzimidazole)], 3.82 (s, 3 H, CH_3N), 3.30 (q, *J* 4.8 Hz, 2 H, CH_2N), 2.61 (t, 2 H, CH_2S), 2.5—1.0 (m, 7 H, CCHC + CCH_2C), 1.09 (s, 3 H, CH_3C), 0.89 (s, 3 H, CH_3C), and 0.69 (s, 3 H, CH_3C). C.d. (MeOH), $\lambda_{max.}$/nm($\Delta\varepsilon$/dm^3 mol^{-1} cm^{-1}): 250 (+2.64), 392 (+2.64), and 450 (−2.36).

HL^3 (Found: C, 67.50; H, 7.90; N, 9.85. Calc. for $C_{24}H_{33}N_3S_2$: C, 67.40; H, 7.75; N, 9.80%). Mass spectrum: *m/z* (%) 428 ([M + 1]$^+$, 43), 427 (M^+, 28), 312 (14), 282 (69), 254 (15), 196 (83), 179 (33), 178 (40), 177 (42), 147 (80), 146 (100), 145 (95), and 131 (33). I.r. (film): 3 300 (br), 3 060w, 2 960s, 2 872m, 1 635s, 1 506m, 1 456s, 1 390m, 1 373m, 1 274m, 1 222m, 1 200m, and 746s cm^{-1}. ^{1}H N.m.r. ($CDCl_3$): δ 11.5 (br m, 1 H, NH), 7.8—7.6 (m, 1 H, Ph–H), 7.4—7.1 (m, 3 H, Ph–H), 6.82 (d, *J* 12.9 Hz, 1 H, =CH), 3.93 [s, 2 H, CH_2C(benzimidazole)], 3.80 (s, 3 H, CH_3N), 3.18 (approximate q, 2 H, CH_2N), 2.55 (approximate t, 2 H, CH_2S), 2.4—1.0 (m, 9 H, CCHC + CCH_2C), 1.09 (s, 3 H, CH_3C), 0.88 (s, 3 H, CH_3C), and 0.70 (s, 3 H, CH_3C). C.d. (MeOH), $\lambda_{max.}$/nm($\Delta\varepsilon$/dm^3 mol^{-1} cm^{-1}): 242 (+2.45), 390 (+2.09), and 445 (−1.91).

Preparation of Zinc(II) *and Copper*(II) *Complexes* (**9**).—To a cold solution (about −10 °C) of the ligand (0.15 mmol) in ethanol (2 cm^3) was added 1 equivalent of methanolic 1 mol dm^{-3} sodium hydroxide followed by a solution of the metal perchlorate salt (0.15 mmol) in ethanol (1 cm^3). A yellow (Zn) or dark green (Cu) precipitate of the complex formed immediately. This was rapidly collected by filtration, washed with small amounts of cold ethanol–water 1:1 (v/v), and dried under vacuum.

[ZnL^1][ClO_4] (Found: C, 46.25; H, 5.50; N, 7.20. Calc. for $C_{22}H_{28}ClN_3O_4S_2Zn$: C, 46.90; H, 5.00; N, 7.45%). I.r. (Nujol mull): 1 622w, 1 584m, 1 494s, 1 340w, 1 286m, 1 100vs, 744m, 721m, and 623s cm^{-1}. ^{1}H N.m.r. (CD_3OD): δ 8.05 (s, 1 H, CH=N), 8.0—7.3 (m, 4 H, Ph–H), 4.23 [s, 2 H, CH_2C(benzimidazole)], 3.94 (s, 3 H, CH_3N), ≈3.9 (m, 2 H, CH_2N), 2.85 (m, 2 H, CH_2S), 2.56 (d, 1 H, ≡CH), 2.3—1.0 (m, 4 H, CCH_2C), 1.17 (s, 3 H, CH_3C), 0.92 (s, 3 H, CH_3C), and 0.82 (s, 3 H, CH_3C). C.d. (MeOH), $\lambda_{max.}$/nm($\Delta\varepsilon$/dm^3 mol^{-1} cm^{-1}): 260 (+1.77), 288 (+1.59), 305 (sh) (+1.15), 356 (−3.15), and 391 (+0.38).

[ZnL^2][ClO_4] (Found: C, 47.50; H, 5.30; N, 6.95. Calc. for $C_{23}H_{30}ClN_3O_4S_2Zn$: C, 47.85; H, 5.25; N, 7.30%). I.r. (Nujol mull): 1 618w, 1 586s, 1 506s, 1 495s, 1 350w, 1 286m, 1 265m, 1 249m, 1 100(br) vs, 752m, 717m, and 625s cm^{-1}. ^{1}H N.m.r. (CD_3OD): δ 7.99 (s, 1 H, CH=N), 8.0—7.3 (m, 4 H, Ph–H), 4.35 [s, 2 H, CH_2C(benzimidazole)], 3.93 (s, 3 H, CH_3N), 3.9 (m, 2 H, CH_2N), 2.75 (m, 2 H, CH_2S), 2.57 (d, 1 H, ≡CH), 2.3—1.0 (m, 6 H, CCH_2C), 1.18 (s, 3 H, CH_3C), 0.92 (s, 3 H, CH_3C), and 0.82 (s, 3 H, CH_3C). C.d. (MeOH), $\lambda_{max.}$/nm($\Delta\varepsilon$/dm^3 mol^{-1} cm^{-1}): 232 (+6.30), 262 (−0.20), 305 (+1.90), 370 (−2.91), and 410 (+ 0.20).

[ZnL^3][ClO_4] (Found: C, 49.50; H, 5.75; N, 7.00. Calc. for $C_{24}H_{32}ClN_3O_4S_2Zn$: C, 48.75; H, 5.45; N, 7.10%). I.r. (Nujol mull): 1 620w, 1 586m, 1 495s, 1 286m, 1 249w, 1 100vs, 745m, 721m, and 623s cm^{-1}. ^{1}H N.m.r. (CD_3OD): δ 7.96 (s, 1 H, CH=N), 8.0—7.2 (m, 4 H, Ph–H), 4.10 [approximate s, 2 H, CH_2C(benzimidazole)], 3.95 (s, 3 H, CH_3N), ≈3.9 (m, 2 H, CH_2N), ≈2.5 (m, 3 H, CCH_2C + ≡CH), 2.3—1.0 (m, 8 H, CCH_2C), 1.15 (s, 3 H, CH_3C), 0.91 (s, 3 H, CH_3C), and 0.81 (s, 3 H, CH_3C). C.d. (MeOH), $\lambda_{max.}$/nm($\Delta\varepsilon$/dm^3 mol^{-1} cm^{-1}): 234 (+13.02), 275 (sh) (+0.91), 323 (+4.72), 373 (−12.90), and 405 (+3.20).

[CuL^1][ClO_4] (Found: C, 46.65; H, 4.95; N, 7.15. Calc. for $C_{22}H_{28}ClCuN_3O_4S_2$: C, 47.05; H, 5.00; N, 7.50%). I.r. (Nujol mull): 1 617w, 1 576m, 1 506m, 1 485s, 1 284m, 1 261m, 1 100(br)vs, 761m, 750s, 719m, and 624s cm^{-1}.

[CuL^2][ClO_4] (Found: C, 47.65; H, 5.05; N, 7.10. Calc. for $C_{23}H_{30}ClCuN_3O_4S_2$: C, 48.00; H, 5.25; N, 7.30%). I.r. (Nujol mull): 1 618w, 1 576m, 1 491s, 1 286m, 1 261m, 1 095(br)vs, 750m, 721w, and 623s cm^{-1}.

[CuL^3][ClO_4] (Found: C, 48.50; H, 5.30; N, 6.95. Calc. for $C_{24}H_{32}ClCuN_3O_4S_2$: C, 48.90; H, 5.45; N, 7.15%). I.r. (Nujol mull): 1 618w, 1 578m, 1 495s, 1 286m, 1 261w, 1 095(br)vs, 746m, 721w, and 623m cm^{-1}.

Preparation of Copper(II) *Complexes* (**11**).—The synthesis of the ligands (**10**) is reported elsewhere.[8] To a cold solution (about −10 °C) of the ligand (0.1 mmol) in ethanol (5 cm^3) were added 2 equivalents of methanolic 1 mol dm^{-3} sodium hydroxide followed by a solution of copper(II) perchlorate hexahydrate (0.1 mmol) in ethanol (2 cm^3). Brown or brownish red precipitates started to form; precipitation was completed by the addition of a few drops of cold water. The product was rapidly filtered off, washed with small amounts of ethanol, and dried under vacuum.

[CuL^4] (Found: C, 60.55; H, 7.05; N, 5.80. Calc. for $C_{24}H_{34}CuN_2S_2$: C, 60.25; H, 7.15; N, 5.85%). I.r. (Nujol mull): 1 634w, 1 580s, 1 495s, 1 286m, 1 253m, 1 054m, and 719m cm^{-1}. C.d. (MeOH), $\lambda_{max.}$/nm($\Delta\varepsilon$/dm^3 mol^{-1} cm^{-1}): 250 (+2.05), 318 (+0.29), 362 (−1.95), 407 (−2.33), 485 (sh) (−0.28), and 600 (−0.08).

[CuL^5] (Found: C, 61.10; H, 7.25; N, 5.60. Calc. for

$C_{25}H_{36}CuN_2S_2$: C, 61.00; H, 7.35; N, 5.70%). I.r. (Nujol mull): 1 624w, 1 586m, 1 493s, 1 286m, 1 267w, 1 060m, and 719m cm^{-1}. C.d. (MeOH), $\lambda_{max.}$/nm($\Delta\varepsilon$/dm^3 mol^{-1} cm^{-1}): 250 (−3.62), 316 (−10.51), 355 (+19.25), 381 (+16.50), 400 (sh), (+13.50), 430 (sh) (−1.20), and 475 (−4.95).

[CuL^6] (Found: C, 65.15; H, 7.00; N, 5.00. Calc. for $C_{30}H_{38}CuN_2S_2$: C, 65.00; H, 6.90; N, 5.05%). I.r. (Nujol mull): 1 620 (sh), 1 574s, 1 483s, 1 286s, 1 241m, 1 108m, 1 085m, 1 073m, 1 033m, 750m, and 725m cm^{-1}. C.d. (MeOH), $\lambda_{max.}$/nm($\Delta\varepsilon$/dm^3 mol^{-1} cm^{-1}): 237 (−16.70), 300 (−13.25), 370 (+32.65), 427 (−11.20), and 475 (−11.33).

Results and Discussion

Ligand Synthesis and Structure.—Models for blue (Type 1) copper sites require co-ordination of thiol, thioether, and imidazole groups in tetrahedral array. Natural product chemistry provides several rigid carbon skeletons that may be potentially useful to obtain ligand molecules with the necessary steric characteristics and we decided to introduce the camphor residue into the synthetic scheme developed for the preparation of the ligands of complexes (**2**).[4b] We initially synthesized (1*R*)-3-mercaptobornan-2-one, (**15**), as the thiol-containing aliphatic equivalent of (**3**), but found insuperable difficulties in the condensation of this compound with the 2-aminothia-alkyl-1-methylbenzimidazoles (**7**). Therefore, we turned to the synthesis of a sulphur-containing camphor residue carrying the more easily conjugable aldehydic group, i.e. (**6**), which became available by formylation of (1*R*)-thiocamphor, (**14**). Condensation of (1*R*)-3-formylthiocamphor with compounds (**7**) afforded the ligands (**8**) according to the synthetic route outlined in the Scheme. The derivatives (**7**) reported here, containing N-methylated benzimidazole nuclei, were preferred to the N-protonated analogues employed earlier[4b] for their practically advantageous much higher solubility in the non-polar solvent mixture required for the condensation with (**6**). The ligands (**10**) were also obtained from the corresponding diamines as described elsewhere.[8]

Like the other β-thioxoketone derivatives,[9] (1*R*)-3-formylthiocamphor can exist as a mixture of tautomers, the most important of which are the intramolecularly hydrogen-bonded *Z*-enol and *Z*-enethiol forms.[8] The presence of several species

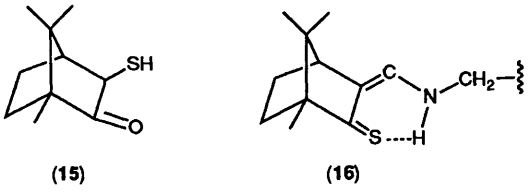

(15) (16)

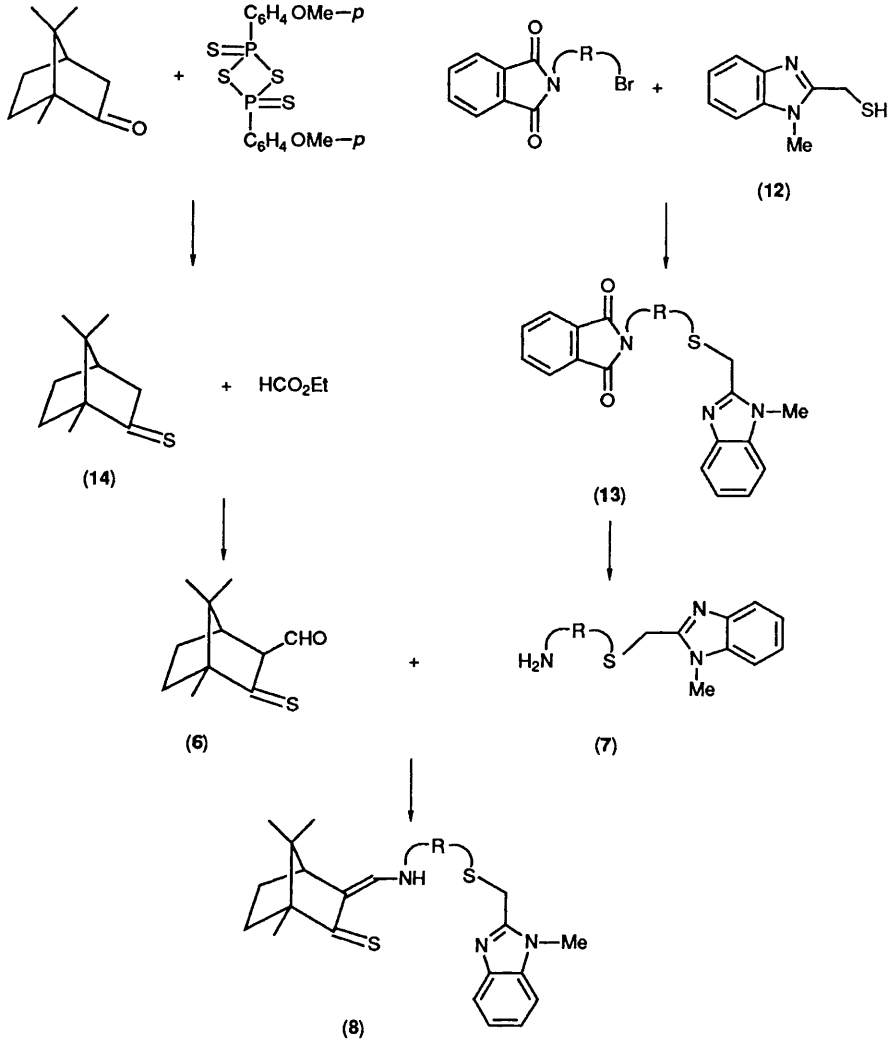

(14) (12) (13) (6) (7) (8)

Scheme. R = $(CH_2)_2$, $(CH_2)_3$, or $(CH_2)_4$

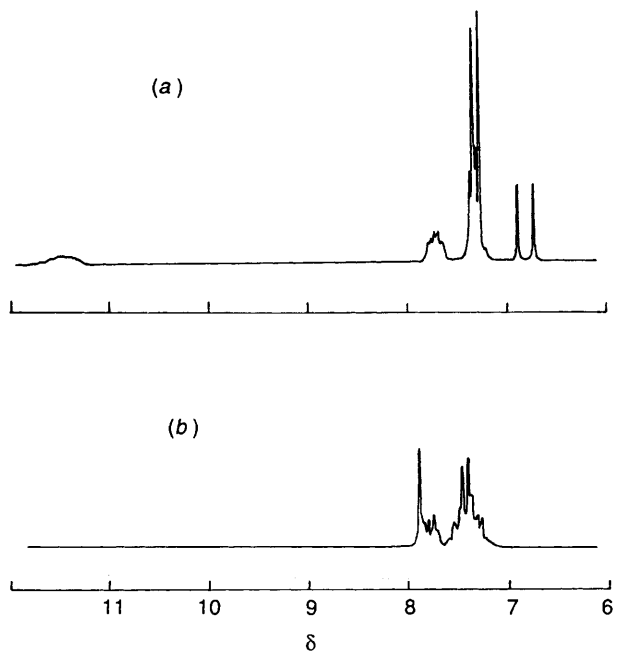

Figure 1. Proton n.m.r. spectra (at 80 MHz) of HL^1 (*a*) and $[ZnL^1][ClO_4]$ (*b*) in $CDCl_3$ solution

and the change in their relative amounts with solvent and with time complicates considerably the interpretation of the spectra of this compound. The spectra data reported here for (**6**) refer to freshly prepared samples. For the ligands (**8**) the situation appears much simpler since only the hydrogen-bonded thioxo-enamine form (**16**) seems to be present. The proton n.m.r. spectra show, for instance, a broad signal at very low field ($\delta \approx 11.5$) for the NH group, a doublet at $\delta \approx 6.8$ for the enamine =CH proton, and a rough quartet structure for the signal at $\delta \approx 3.3$, associated with the nitrogen-bonded methylene group. Decoupling experiments have shown the connections between these groups. The large coupling constant ($J \approx 13$ Hz) between the enamine =CH and the NH protons indicates their *trans* arrangement in structure (**16**) (Figure 1).

As shown in this Figure for $[ZnL^1]^+$, binding of the ligands (**8**) to zinc(II) occurs in their enethiolateimine form: the doublet at $\delta \approx 6.8$ of the free ligand is replaced by a signal at $\delta \approx 8.0$ for the imine proton and also the signal of the nitrogen-bonded methylene group moves downfield (from $\delta \approx 3.3$ to ≈ 3.9), due to the double-bond character of the adjacent azomethine group. The enethiolateimine nature of the ligands in complexes (**9**) is also shown by the comparison of the electronic (Table 1) and c.d. spectra of (**8**) and (**9**). The intense absorption band of the ligand at ≈ 400 nm, associated with the lowest-energy $\pi \longrightarrow \pi^*$ transition of the thioxoenamine chromophore, undergoes a blue shift in the zinc(II) (≈ 380 nm) and copper(II) (≈ 370 nm) complexes, in agreement with the predominant enethiolateimine character of the ligand chromophore in these species. This trend in the optical spectra is well established in the tautomeric equilibria involving ketoenamine and enolimine forms[10] and parallels the behaviour described previously for the imines derived from (**3**) and their metal complexes.[4,7]

Spectroscopic Properties of Copper(II) Complexes.—The copper(II) complexes (**9**) with HL^1–HL^3 are rather redox unstable in solution at room temperature but could be isolated in reasonable purity by performing their synthesis at low temperature, where ready precipitation occurs. In the solid state the compounds appear reasonably stable. The instability in solution increases in the order $[CuL^1]^+ \ll [CuL^2]^+ < [CuL^3]^+$ and has prevented so far the collection of crystalline materials suitable for a complete structural characterization. Since solutions of $[CuL^2]^+$ and $[CuL^3]^+$ decompose rapidly even at low temperature we recorded the low-energy portion of their electronic spectra in the presence of small amounts of added ligand. This procedure yielded a sufficiently high concentration of the complexes for the (short) time required to record the spectra with the diode-array spectrophotometer and so locate the low-energy ligand-to-metal charge-transfer (l.m.c.t.) and *d–d* bands, even though the observed intensity of these bands is clearly lower than expected if the concentration of copper(II) were to correspond to the total copper present.

Besides the intraligand absorptions, which can be identified by examining the electronic spectra of the zinc(II) complexes, the near-u.v. and visible spectra of $[CuL^1]^+$–$[CuL^3]^+$ contain moderately intense c.t. bands and somewhat weaker *d–d* bands (Table 1). Of the possible l.m.c.t. transitions, those originating from the imine,[4a,11] thioether,[12] and benzimidazole[13] groups should not contribute significantly to the electronic spectrum of the complexes above 400 nm. Alcoholic solutions of the 2-aminothia-alkyl-1-methylbenzimidazoles (**7**) with copper(II) in 1:1 ratio exhibit only broad and featureless absorptions in the range 300—400 nm ($\varepsilon \approx 1\,500$ dm^3 mol^{-1} cm^{-1}). In the spectra of $[CuL^1]^+$–$[CuL^3]^+$, therefore, the absorptions associated with these l.m.c.t. transition occur unresolved under the more intense low-energy bands of the ligands. The medium-intensity band between 410 and 435 nm ($\varepsilon \gtrsim 3\,500$ dm^3 mol^{-1} cm^{-1}) in the spectra of the complexes originates from the enethiolate sulphur donor and can be attributed to the $\sigma(S^-) \longrightarrow Cu^{II}$ l.m.c.t. transition. The much lower intensity $\pi(S^-) \longrightarrow Cu^{II}$ l.m.c.t. transition is located in the range 520—535 nm ($\varepsilon \gtrsim 1\,200$ dm^3 mol^{-1} cm^{-1}) and partially overlaps with the ligand-field band occurring in the range 610—650 nm. Although the intensity of this ligand-field band appears unusually high ($\varepsilon \gtrsim 1\,500$ dm^3 mol^{-1} cm^{-1}) it can be enhanced by intensity-borrowing from the intense $\sigma(S^-) \longrightarrow Cu^{II}$ l.m.c.t. transition. It is also apparent that all the visible absorption bands undergo progressive red shifts in the series $[CuL^1]^+$–$[CuL^3]^+$; unfortunately, the instability in solution of these compounds prevents a satisfactory analysis of the intensity change accompanying the energy shifts.

The complexes $[CuL^4]$–$[CuL^6]$, (**11**), are much more redox stable than $[CuL^1]^+$–$[CuL^3]^+$ in solution and their optical spectral data in Table 1 are fully quantitative. The low-energy intraligand absorptions for these bis(enethiolateimine) complexes can be associated with the intense near-u.v. bands between 320 and 360 nm. As before, if we neglect the weak imine $\pi(N) \longrightarrow Cu^{II}$ l.m.c.t. transitions, buried under the intense absorptions in the range 350—400 nm, all the remaining optical bands are due to thiolate to Cu^{II} l.m.c.t. and ligand-field transitions. Using the $\sigma(S^-) \longrightarrow Cu^{II}$ and $\pi(S^-) \longrightarrow Cu^{II}$ notation to indicate the higher intensity and lower intensity, respectively, of the observed l.m.c.t. bands, the absorption shift from 384 nm, for $[CuL^4]$, to 425 nm, for $[CuL^6]$, is assigned to the $\sigma(S^-) \longrightarrow Cu^{II}$ combination and that shifting from 420 to 490 nm to the $\pi(S^-) \longrightarrow Cu^{II}$ combination of l.m.c.t. transitions. These bands are approximately twice as intense as the corresponding bands for the $[CuL^1]^+$–$[CuL^3]^+$ series. The bands at low energies, 500—590 nm, are assigned to ligand-field transitions, although again their intensity is remarkably high. Actually, the shape of the absorption curve of the complex $[CuL^4]$ indicates the presence of an additional, somewhat weaker absorption with a maximum above 800 nm, due to low-energy ligand-field components, and it is likely that $[CuL^5]$ and $[CuL^6]$ will exhibit corresponding absorptions at still lower energies, outside the range covered by our instrument (200—800 nm). In general, it is clear that an increase in intensity accompanies the red shift of the l.m.c.t. and *d–d* bands in the

Table 1. Electronic spectra of ligands (**8**), and zinc(II) and copper(II) complexes (**9**) and (**11**) in methanol solution

Compound	$\lambda_{max.}$/nm (ε/dm^3 mol^{-1} cm^{-1})
HL^1	257 (8 900), 270 (sh) (7 700), 278 (7 000), 286 (5 500), 402 (15 500), 450 (sh) (500)
HL^2	257 (9 300), 270 (sh) (7 650), 278 (7 350), 286 (6 100), 400 (15 300), 450 (sh) (500)
HL^3	258 (9 000), 270 (sh) (7 600), 280 (7 100), 288 (6 000), 401 (13 000), 450 (sh) (400)
$[ZnL^1][ClO_4]$	242 (11 100), 278 (9 800), 285 (sh) (8 100), 382 (10 800)
$[ZnL^2][ClO_4]$	242 (11 400), 274 (8 900), 280 (9 100), 382 (10 800)
$[ZnL^3][ClO_4]$	244 (12 800), 278 (10 800), 285 (sh) (9 400), 382 (11 100)
$[CuL^1][ClO_4]$[a]	245 (15 500), 274 (14 000), 282 (12 400), 366 (12 300), 410 (4 700), 520 (sh), (1 550), 610 (1 700)
$[CuL^2][ClO_4]$[a]	240 (sh) (13 500), 276 (14 100), 282 (14 200), 370 (8 800),[b] 430 (sh) (3 500),[b] 525 (sh) (900),[b] 650 (1 200)[b]
$[CuL^3][ClO_4]$[a]	240 (sh) (13 500), 276 (13 700), 280 (12 000), 370 (6 100),[b] 435 (4 000),[b] 530 (1 350),[b] 650 (1 500)[b]
$[CuL^4]$	238 (20 500), 324 (13 000), 350 (7 800), 384 (6 900), 420 (sh) (3 600), 500 (sh) (1 200)
$[CuL^5]$	232 (19 800), 332 (9 000), 354 (7 600), 410 (5 000), 480 (2 800), 560 (sh) (1 800)
$[CuL^6]$	265 (sh) (18 000), 340 (sh) (16 000), 352 (17 000), 425 (11 000), 490 (4 500), 590 (sh) (3 000)

[a] Spectra recorded at about 0 °C. [b] This band decreases extremely rapidly in intensity even at low temperatures and in the presence of excess of ligand.

Table 2. E.p.r. spectral results for copper(II) complexes in frozen ethanol–chloroform solutions at −150 °C

Compound	$g_{\parallel}$	$10^4\lvert A_{\parallel}\rvert$/cm^{-1}	$g_{\perp}$
$[CuL^1][ClO_4]$	2.178	160	2.03
$[CuL^2][ClO_4]$*	2.140	135	2.03
$[CuL^3][ClO_4]$*	2.142	130	2.03
$[CuL^4]$	2.113	175	2.02
$[CuL^5]$	2.116	153	2.02
$[CuL^6]$	2.130	144	2.03

* Recorded in the presence of added ligand.

series $[CuL^4]$–$[CuL^6]$ (the apparent higher absorptions coefficient for the l.m.c.t. bands of $[CuL^4]$ with respect to those of $[CuL^5]$ depends on their overlap with the adjacent absorptions at higher energy).

An interesting feature which parallels this optical behaviour is the remarkable increase in the optical activity of the complexes from $[CuL^4]$ to $[CuL^6]$. The most intense c.d. bands correspond to the intraligand $\pi \longrightarrow \pi^*$ transitions of the enethiolateimine chromophores and it is likely that this optical activity originates from coupling of the transition moments of the chromophores localized in the two halves of the molecules. The increase in optical activity in the series $[CuL^4]$–$[CuL^6]$ then depends on the distortion of the copper(II) chromophore which accompanies the lengthening of the carbon chain R'. Unfortunately, the instability in solution prevents the recording of reliable c.d. spectra for $[CuL^1]^+$–$[CuL^3]^+$, due to the relatively long time required

The e.p.r. parameters for the copper(II) complexes (**9**) and (**11**) obtained from frozen-solution spectra are collected in Table 2. In general, all the spectra were of the axial or nearly axial type ($g_{\parallel} > g_{\perp}$, large $\lvert A_{\parallel}\rvert$ values) and allowed accurate determination of the parallel components of the spin-Hamiltonian parameters $g_{\parallel}$ and $A_{\parallel}$, while precise values of the perpendicular components are difficult to obtain without appropriate simulation of the spectra. The most salient feature of the e.p.r. spectra, common to the two series $[CuL^1]^+$–$[CuL^3]^+$ and $[CuL^4]$–$[CuL^6]$, is the marked reduction in $\lvert A_{\parallel}\rvert$ as the length of the carbon chains R and R' increases. The $g_{\parallel}$ values are generally higher and the $\lvert A_{\parallel}\rvert$ values lower in the $[CuN_2SS^*]^+$ series than in the $[CuN_2S_2]^0$ series because the former complexes carry a positive charge and the latter contain two chelate rings with extended π systems and thus high covalent character in the coordinate bonds. Low values of the hyperfine constant $\lvert A_{\parallel}\rvert$ indicate significant pseudo-tetrahedral distortion of the copper(II) chromophore[14] and we note that the $\lvert A_{\parallel}\rvert$ value found here for $[CuL^3]^+$ compares favourably with the lowest ones that have been reported so far for synthetic copper(II) thiolate complexes, *i.e.* those for the systems (**17**)[6b] and (**18**).[6c]

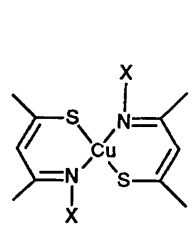

(17)

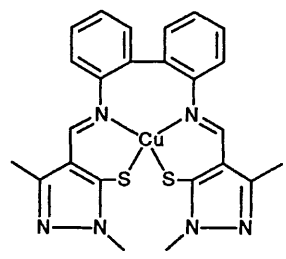

(18)

X = *p*– MeC_6H_4 or cyclohexyl

The $\lvert A_{\parallel}\rvert$ values found here for the complex $[CuL^6]$ is somewhat higher than that of (**18**), even though the two compounds have the same chelate ring systems and charge. Apparently the rigidity of the biphenyl bridge between the two imine nitrogens has a positive effect in enhancing a pseudo-tetrahedral distortion at the copper(II) centre. The same result is obtained in $[CuL^3]^+$, with a flexible four-carbon atom bridge, by the inclusion of the smaller and more rigid five-membered chelate ring between the thioether and benzimidazole donors, as shown by our previous investigation on complexes (**2**).[4b]

The e.p.r. parameters of $[CuL^1]^+$ are indicative of a square-pyramidal five-co-ordinate species, with a solvent molecule bound in axial position. This tendency to five-co-ordination of the systems with a chain R of two carbon atoms is also a consequence of the small benzimidazole chelate ring, as discussed in more detail for the corresponding member in the series (**2**).[4b] A major difference between the series (**2**) and (**9**), however, is found in the behaviour of the complexes containing a chain R with three carbon atoms. The pyridinethiolate complex is trigonal bipyramidal,[4b] while the enethiolate complex $[CuL^2]^+$ is pseudo-tetrahedral. It is likely that the dipositive charge of the pyridinethiolate complex makes the copper(II) centre too hard to bind strongly to an equatorial thioether, so that this group prefers to occupy the weaker axial co-ordination position.

Electrochemistry of Copper(II) Complexes.—As mentioned above, the copper(II) complexes (**9**) are not long-lived in solution, so that their electrochemistry in acetonitrile solution has been explored at −15 °C. Figure 2 show a cyclic voltammogram recorded at a platinum electrode on an acetonitrile solution of $[CuL^1]^+$. The reduction process occurring at peak A is directly associated with reoxidation peak B in the reverse scan. By contrast, an ill shaped irreversible reducton step takes place at more negative potentials (E_p = −1.24 V), as well as an irreversible anodic oxidation at positive potentials (E_p = +1.05 V). Controlled-potential coulometric tests performed at −15 °C on the reduction step illustrated in Figure 2 (E_w = −0.3 V) indicated the consumption of one electron per

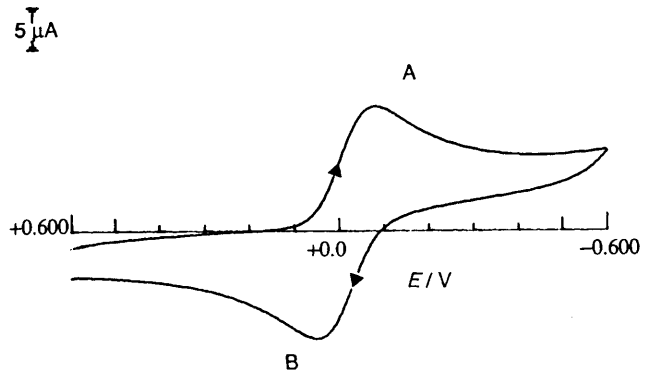

Figure 2. Cyclic voltammogram recorded at a platinum electrode for a deaerated acetonitrile solution containing $[CuL^1]^+$ (2.1×10^{-3} mol dm^{-3}) and $[NEt_4][ClO_4]$ (0.1 mol dm^{-3}). Scan rate 0.2 V s^{-1}, −15 °C

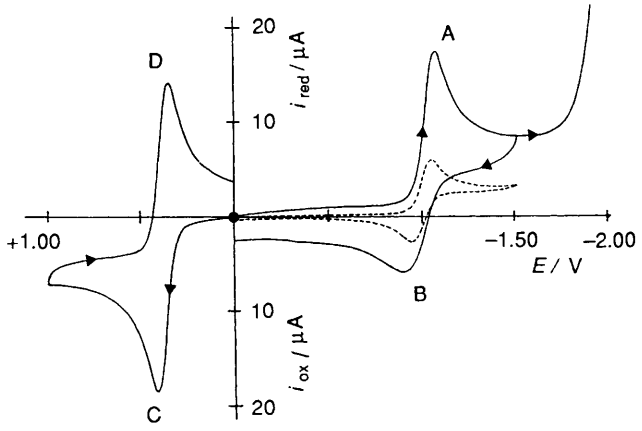

Figure 3. Cyclic voltammograms recorded at a platinum electrode for an acetonitrile solution containing $[CuL^4]$ (2.2×10^{-3} mol dm^{-3}) and $[NEt_4][ClO_4]$ (0.1 mol dm^{-3}) at 18 °C. Scan rates: (——) 0.2 and (----) 0.02 V s^{-1}.

Table 3. Electrochemical characteristics of the redox changes exhibited by the copper(II) complexes (**9**) and (**11**) in acetonitrile solution

	Cu^{III}–Cu^{II}		Cu^{II}–Cu^{I}		Cu^{I}-Co^{0}
Compound	E^0/V	ΔE_p[a]/mV	E^0/V	ΔE_p[a]/mV	E_p[b]/V
$[CuL^1]^+$	+1.05[b–d]	—	−0.02[d]	96[d]	−1.24[b–d]
	—	—	0.00[e]	88[e]	—
$[CuL^2]^+$	+1.09[b–d]	—	−0.02[d]	86[d]	−1.27[b–d]
	—	—	−0.01[e]	84[e]	—
$[CuL^4]$	+0.36[d]	58[d]	−1.12[c,d]	—	—
	+0.37[e]	59[e]	−1.03[e]	100[e]	—
$[CuL^5]$	+0.43[d,f]	78[b,d]	−0.96[c,d]	—	—
	+0.44[e,f]	85[b,e]	−0.84[e]	116[e]	—
$[CuL^6]$	+0.50[b–d]	—	−0.71[d,f]	102[d]	—
	+0.47[b,c,e]	—	−0.71[e,f]	84[e]	—

[a] Measured at 0.02 V s^{-1}. [b] Measured at 0.2 V s^{-1}. [c] Peak potential for irreversible process. [d] At −15 °C. [e] At +18 °C. [f] Complicated by slow decomposition.

molecule. The dark green solution of the copper(II) species turns yellow and displays a cyclic voltammogram complementary to that shown in Figure 2, thus showing the full chemical reversibility of the Cu^{II}–Cu^{I} couple.

Analysis[15] of the cyclic voltammetric response A/B at scan rates varying from 0.02 to 10.24 V s^{-1} indicates that: (*i*) the ratio $i_{p(B)}/i_{p(A)}$ is constantly equal to unity; (*ii*) the current function $i_{p(A)}\,v^{-\frac{1}{2}}$ decreases by less than 10%; the peak-to-peak separation E_p progressively increases from 96 to 213 mV. Under the same experimental conditions, the nominally reversible one-electron oxidation of ferrocene displays an increase of ΔE_p from 63 to 148 mV. These data are diagnostic for an electrochemically quasi-reversible $[CuL^1]^+$–$[CuL^1]$ electron transfer. A qualitatively similar redox pattern is exhibited by $[CuL^2]^+$. Unfortunately, $[CuL^3]^+$ decomposed so quickly even at −15 °C that we could not test its redox propensity, while it was possible to test briefly the electrochemical behaviour of $[CuL^1]^+$ and $[CuL^2]^+$ even at +18 °C, within a few seconds of dissolution.

The redox potentials of the complexes now discussed are reported in Table 3, together with those relevant to the derivatives of type (**11**), which will be discussed below. Also reported are the peak-to-peak separations ΔE_p at slow scan rate (0.02 V s^{-1}) for redox systems having features of chemical reversibility. In the absence of either uncompensated solution resistances or anomalous electrode surface effects, the marked departure of ΔE_p from 59 mV, theoretically predicted for a purely reversible electron transfer, can be qualitatively assumed as an index of the occurrence of significant geometrical reorganizations accompanying the redox change.[16] It is not unexpected that the couple $[CuL^1]^+$–$[CuL^1]$ experiences some significant reorganizational barrier in view of the likely rearrangement from square-pyramidal Cu^{II} to pseudo-tetrahedral Cu^{I}. In contrast, the electrochemical parameters cannot be taken to support the spectroscopic evidence assigning a pseudo-tetrahedral geometry to $[CuL^2]^+$, in that the differences with respect to $[CuL^1]^+$ are not sufficiently significant, even if they are suggestive of this.

Figure 3 shows the cyclic voltammetric behaviour of $[CuL^4]$ in acetonitrile solution at room temperature. The complex undergoes an anodic process at peak C and a cathodic process at peak A, each displaying a directly associated response in the reverse scan (peaks D and B, respectively). Controlled-potential coulometry on peak C (E_w = +0.6 V) consumes 1 F mol^{-1}. Correspondingly the initially red-brown solution turns to lemon-yellow, displaying a cyclic voltammogram simply reversed with respect to that of Figure 3. Exhaustive reduction at peak A (E_w = −1.3 V) also consumes 1 F mol^{-1}, yielding a golden solution which displays a cyclic voltammogram complementary to the initial one.

These data indicate both a chemically reversible one-electron oxidation and a chemically reversible one-electron reduction. Analysis of the peak system C/D with scan rate conforms to an electrochemically reversible Cu^{II}–Cu^{III} redox change. However, some complication arises with the A/B peak system. As is well discernible in Figure 3, the ratio $i_{p(B)}/i_{p(A)}$ is equal to unity at 0.02 V s^{-1} but decreases with scan rate (0.6:1 at 0.2 V s^{-1}). Since such behaviour holds also at a mercury electrode as well as in dimethyl sulphoxide solution, it seems likely that we can discard interfacial effects. This being the case, the only electrode mechanism which can be invoked is the occurrence of an equilibrium reaction following the electron transfer:[15]

$$[CuL^4] \underset{-e}{\overset{+e}{\rightleftharpoons}} [CuL^4]^- \underset{k_b}{\overset{k_f}{\rightleftharpoons}} [CuL^{4*}]^-.$$

We do not know the real structural features of the equilibrium component $[CuL^{4*}]^-$, but, speculatively, some bond breaking/making in the co-ordination sphere of copper(I) seems likely. For instance, the copper(II)–copper(I) reduction in some pentathia- and hexathia-macrocyclic complexes is chemically reversible, but accompanied by bond breaking from one sulphur co-ordinating site.[17,18] Since decreasing the temperature or increasing the scan rate have the same kinetic effects upon electrode processes, cyclic voltammograms concerning the peak system A/B at −15 °C show an $i_{p(B)}/i_{p(A)}$ ratio notably lower than unity even at 0.02 V s^{-1}. Such a behaviour is characteristic for the Cu^{II}–Cu^{I} reduction of $[CuL^5]$ and $[CuL^6]$ too.

A different behaviour is observed for the Cu^{II}–Cu^{III} oxidation. The one-electron oxidation of $[CuL^5]$ is complicated by decomposition of $[Cu^{III}L^5]^+$. As expected, at −15 °C the lifetime of $[CuL^5]^+$ ($t_{\frac{1}{2}} \approx 2.5$ s) is longer than that at +18 °C ($t_{\frac{1}{2}} \approx 0.5$ s). By contrast, the oxidation of $[CuL^6]$ is totally irreversible in character at both −15 and +18 °C. The redox potentials of the electron transfer for the complexes of type (**11**) are summarized in Table 3.

The stability of the copper(III) complex $[CuL^4]^+$ with respect to the other complexes is strongly indicative of the complete planarity of its CuN_2S_2 core.[7b,16] The increase in length of the bridging carbon chain introduces a slight distortion in the case of $[CuL^5]$, making only transient the relevant copper(III) species, while it definitively induces departure from planarity in $[CuL^6]$, as well as in $[CuL^1]^+$ and $[CuL^2]^+$.

A final comment is merited by the fact that the potentials of the Cu^{II}–Cu^{I} couple for complexes (**11**) are notably more negative than those of complexes (**9**). Beyond any doubt, the formylthiocamphor fragment is more saturated than a pyridinethione fragment so that complexes (**9**) have a Cu^{II}–Cu^{I} redox potential 0.3 V on average more negative than that of the corresponding complexes (**1**) and (**2**).[4b] Nevertheless, the difference of about 1 V between the redox potentials of complexes (**11**) and those of the corresponding complexes (**4**) is likely attributable not only to inductive electronic factors but also to coulombic effects due to the fact that complexes (**4**) are doubly charged cations whereas (**11**) are neutral. This means that the difference in potential between (**11**) and (**9**) has a significant contribution also from the difference in the overall charge.

Conclusion

The spectral properties of the systems (**9**) and (**11**) show that a significant degree of tetrahedral distortion at Cu^{II} can be imposed by lengthening of the carbon chains R and R′. Although, in general, the spectroscopic properties of the protein blue sites [$\sigma(S^-) \longrightarrow Cu^{II}$ l.m.c.t. at *ca.* 600 nm, $\pi(S^-) \longrightarrow Cu^{II}$ at *ca.* 750 nm, and $|A_{\parallel}| < 100 \times 10^{-4}$ cm^{-1}][19] are still somewhat far from being matched by the model complexes, we note that the shift of the l.m.c.t. bands towards the red[6d] and the decrease in the $|A_{\parallel}|$ value[14c] change more than linearly with the degree of tetrahedral twist away from the square-planar configuration of the copper(II) centre. Therefore, we expect that a further moderate distortion towards the tetrahedral environment, induced in systems of type (**9**), perhaps increasing the rigidity of the chain R, will produce a more significant approach to the optical and e.p.r. parameters that characterize the blue sites. On the other hand, the redox potential of the Cu^{II}–Cu^{I} couples for the model systems reported lie in the range displayed by the blue sites (from −0.1 to +0.5 V *vs.* s.c.e.),[14c] showing that the extent of tetrahedral distortion at the metal is not so critical in determining the accessibility to the range of protein redox couples.

Acknowledgements

The authors thank the Italian Ministero della Pubblica Istruzione for financial support and M. Bonfà for recording n.m.r. spectra.

References

1 P. M. Colman, H. C. Freeman, J. M. Guss, M. Murata, V. A. Norris, J. A. M. Ramshaw, and M. P. Venkatappa, *Nature (London)*, 1978, **272**, 319; E. T. Adman, R. E. Stenkamp, L. C. Sieker, and L. H. Jensen, *J. Mol. Biol.*, 1978, **123**, 35; E. T. Adman and L. H. Jensen, *Isr. J. Chem.*, 1981, **21**, 8; G. E. Norris, B. F. Anderson, and E. N. Baker, *J. Am. Chem. Soc.*, 1986, **108**, 2784; E. T. Adman, S. Turley, R. Branson, K. Petratos, D. Banner, D. Tsernoglou, T. Beppu, and H. Watanabe, *J. Biol. Chem.*, 1989, **264**, 87; A. Messerschmidt, A. Rossi, R. Ladenstein, R. Huber, M. Bolognesi, G. Gatti, A. Marchesini, R. Petruzzelli, and A. Finazzi-Agrò, *J. Mol. Biol.*, 1989, **206**, 513.

2 J. S. Thompson, T. J. Marks, and J. A. Ibers, *Proc. Natl. Acad. Sci. USA*, 1977, **74**, 3114; *J. Am. Chem. Soc.*, 1979, **101**, 4180; O. P. Anderson, C. M. Perkins, and K. K. Brito, *Inorg. Chem.*, 1983, **22**, 1267; E. John, P. K. Bharadwaj, J. A. Potenza, and H. J. Schugar, *ibid.*, 1986, **25**, 3065.

3 J. M. Downes, J. Whelan, and B. Bosnich, *Inorg. Chem.*, 1981, **20**, 1081; J. Whelan and B. Bosnich, *ibid.*, 1986, **25**, 3671.

4 (*a*) L. Casella, *Inorg. Chem.*, 1984, **23**, 2781, 4781; (*b*) L. Casella, M. Gullotti, A. Pintar, F. Pinciroli, R. Viganò, and P. Zanello, *J. Chem. Soc., Dalton Trans.*, 1989, 1161.

5 J. Becher, D. J. Brockway, K. S. Murray, P. J. Newman, and H. Toftlund, *Inorg. Chem.*, 1982, **21**, 1791.

6 (*a*) J. Becher, H. Toftlund, and P. H. Olesen, *J. Chem. Soc., Chem. Commun.*, 1983, 740; (*b*) P. Beardwood and J. F. Gibson, *ibid.*, p. 1099; (*c*) O. P. Anderson, J. Becher, H. Frydendhal, L. F. Taylor, and H. Toftlund, *ibid.*, 1986, 699; (*d*) H. Toftlund, J. Becher, P. H. Olesen, and J. Z. Pedersen, *Isr. J. Chem.*, 1985, **25**, 56; (*e*) J. Becher, H. Toftlund, P. H. Olesen, and H. Nissen, *Inorg. Chim. Acta*, 1985, **103**, 167.

7 (*a*) L. Casella, M. Gullotti, and R. Viganò, *Inorg. Chim. Acta*, 1986, **124**, 121; (*b*) M. Gullotti, L. Casella, A. Pintar, E. Suardi, P. Zanello, and S. Mangani, *J. Chem. Soc., Dalton Trans.*, 1989, 1979.

8 L. Casella, M. Gullotti, M. Sisti, and R. Pagliarin, unpublished work.

9 J. Emsley, *Struct. Bonding (Berlin)*, 1984, **57**, 147.

10 See, for example, L. Casella and M. Gullotti, *J. Am. Chem. Soc.*, 1983, **105**, 803; L. Casella, M. Gullotti, and A. Rockenbauer, *J. Chem. Soc., Dalton Trans.*, 1984, 1033.

11 L. Casella and M. Gullotti, *Inorg. Chem.*, 1983, **22**, 2259; L. Casella, M. Gullotti, and G. Pacchioni, *J. Am. Chem. Soc.*, 1982, **104**, 2386.

12 A. R. Amundsen, J. Whelan, and B. Bosnich, *J. Am. Chem. Soc.*, 1977, **99**, 6730; V. M. Miskowski, J. A. Thich, R. Solomon, and H. J. Schugar, *ibid.*, 1976, **98**, 8344; A. W. Addison, T. N. Rao, J. Reedijk, J. van Rijn, and G. C. Verschoor, *J. Chem. Soc., Dalton Trans.*, 1984, 1349.

13 E. E. Bernaducci, P. K. Bharadwaj, R. A. Lalancette, K. Krogh-Jespersen, J. A. Potenza, and H. J. Schugar, *Inorg. Chem.*, 1983, **22**, 3911; J. V. Dagdigian, V. McKee, and C. A. Reed, *ibid.*, 1982, **21**, 1332; A. W. Addison, P. J. Burke, K. Henrick, T. N. Rao, and E. Sinn, *ibid.*, 1983, **22**, 3645.

14 (*a*) H. Yokoi and A. W. Addison, *Inorg. Chem.*, 1977, **16**, 1341; (*b*) U. Sakaguchi and A. W. Addison, *J. Chem. Soc., Dalton Trans.*, 1979, 600; (*c*) A. W. Addison, in 'Copper Coordination Chemistry: Biochemical and Inorganic Perspectives,' eds. K. D. Karlin and J. Zubieta, Adenine Press, New York, 1983, p. 109.

15 E. R. Brown and J. Sandifer, in 'Physical Methods of Chemistry, Electrochemical Methods,' eds. B. W. Rossiter and J. F. Hamilton, Wiley, New York, 1986, vol. 2, ch. 4.

16 P. Zanello, *Comments Inorg. Chem.*, 1988, **8**, 45; in 'Stereochemistry of Organometallic and Inorganic Compounds,' ed. I. Bernal, Elsevier, Amsterdam, 1990, vol. 4, in the press.

17 P. W. R. Corfield, C. Ceccarelli, M. D. Glick, I. W-Y. Moy, L. A. Ochrymowycz, and D. B. Rorabacher, *J. Am. Chem. Soc.*, 1985, **107**, 2399.

18 J. A. R. Hartman and S. R. Cooper, *J. Am. Chem. Soc.*, 1986, **108**, 1202.

19 H. B. Gray and E. I. Solomon, in 'Copper Proteins,' ed. T. G. Spiro, Wiley, New York, 1981, p. 1.

Received 14*th February* 1990; *Paper* 0/00696C